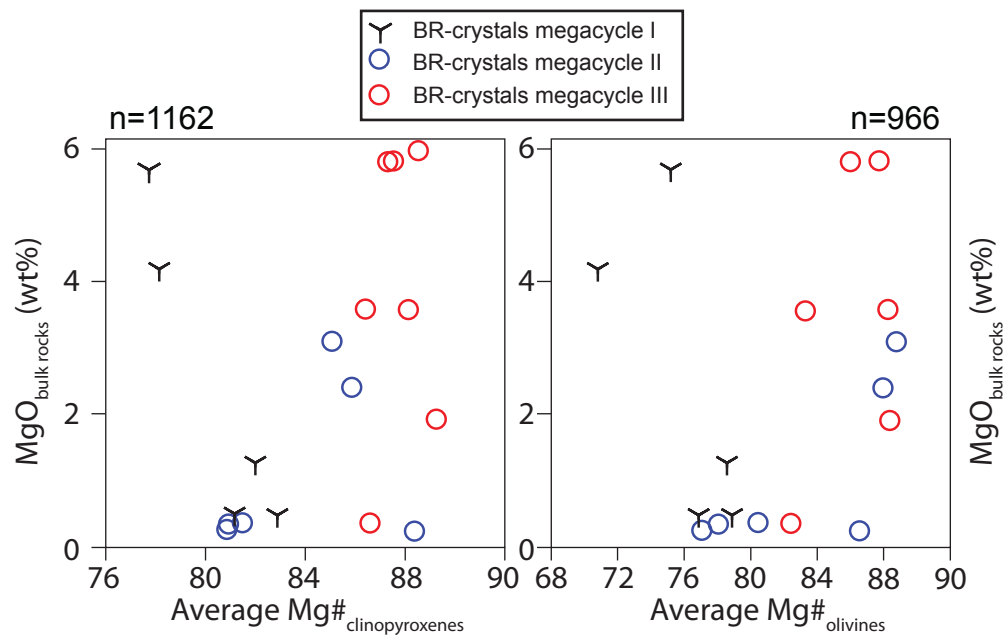
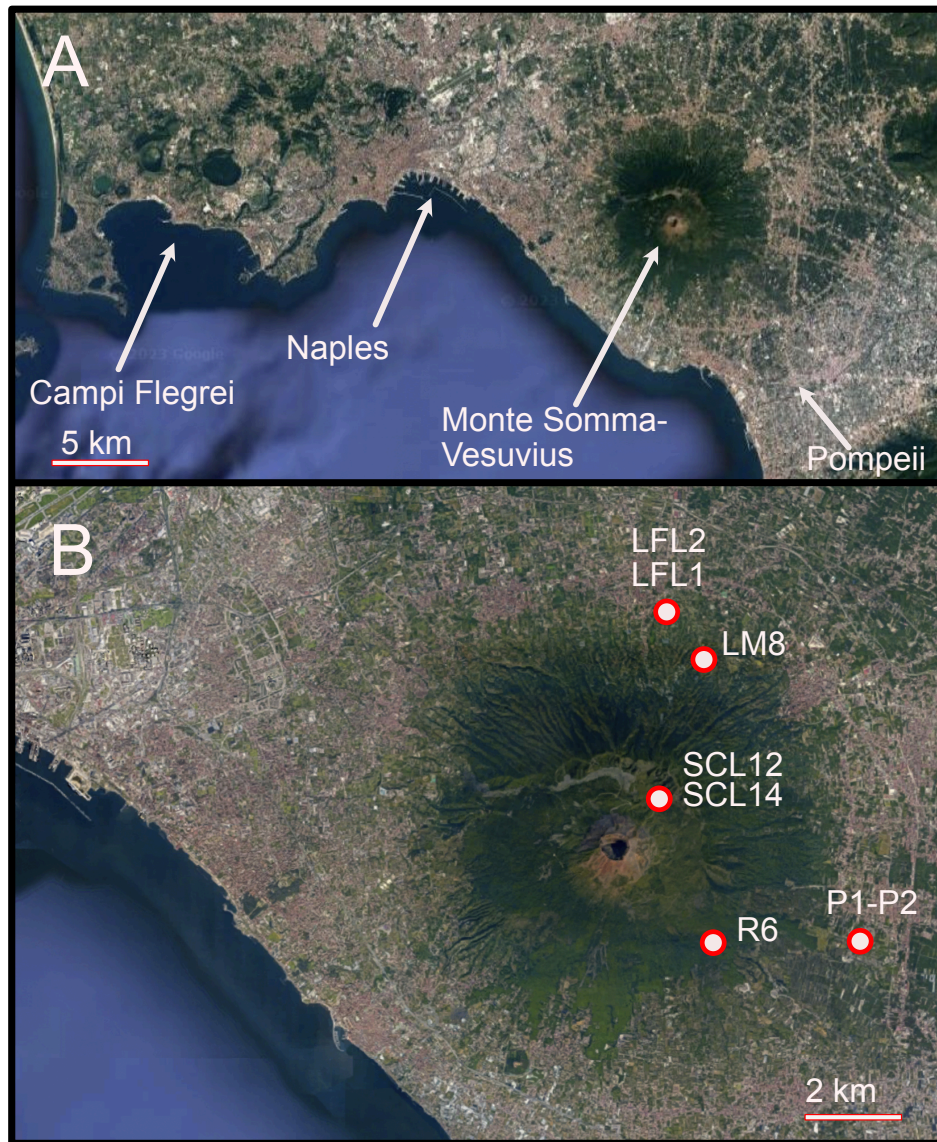


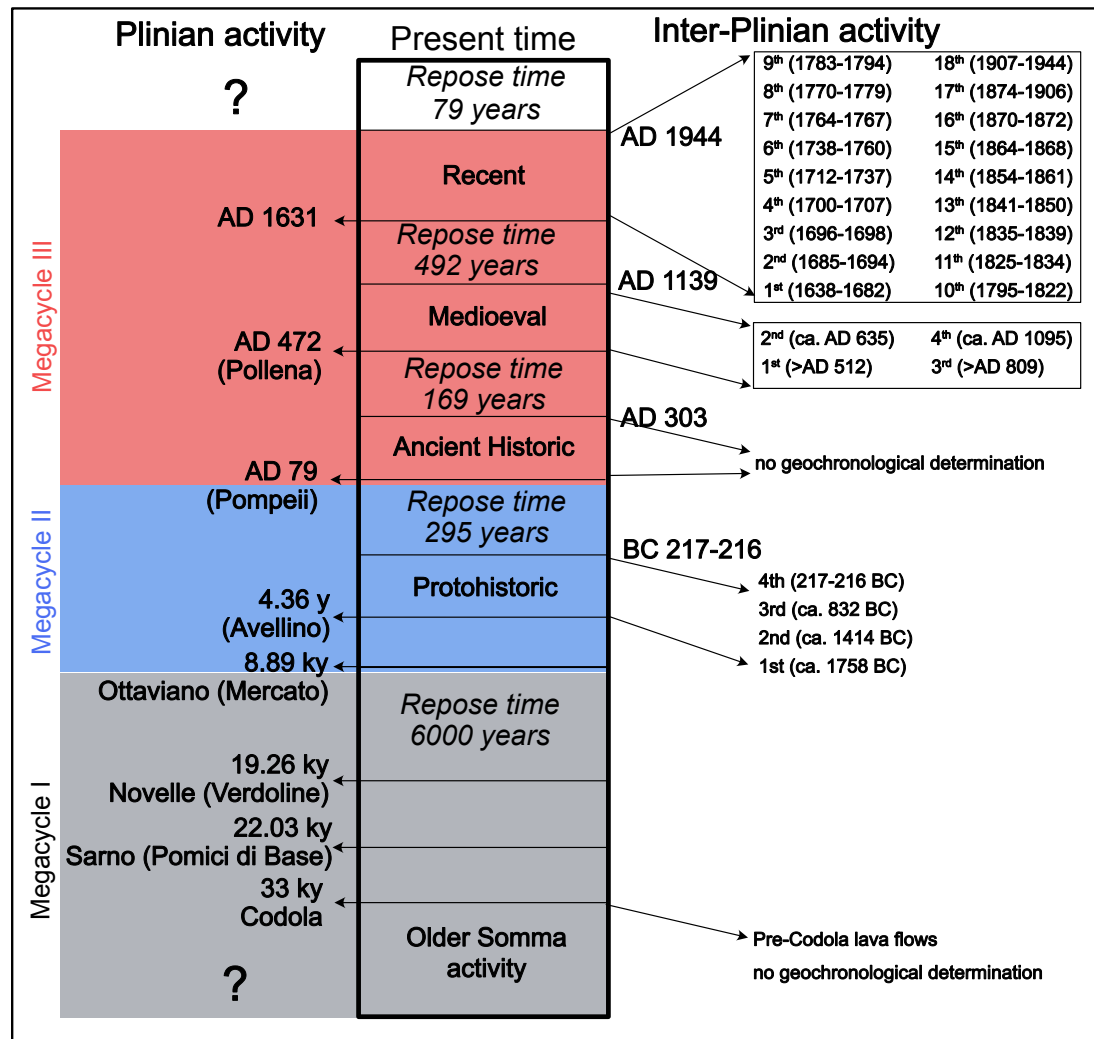
Supplementary Figures and Captions



Supplementary Figure S1. Bulk rock (BR)-phenocryst disequilibrium. Panel a) Average Mg# of clinopyroxenes versus MgO of BR discriminated by megacycles and eruption style. Panel b) Average Mg# of olivine versus MgO of BR discriminated by megacycles and eruption style. Data from Redi et al. (2017). Note the lack of correlation in the two diagrams. Megacycles are based on classification proposed by Ayuso et al. (1998).



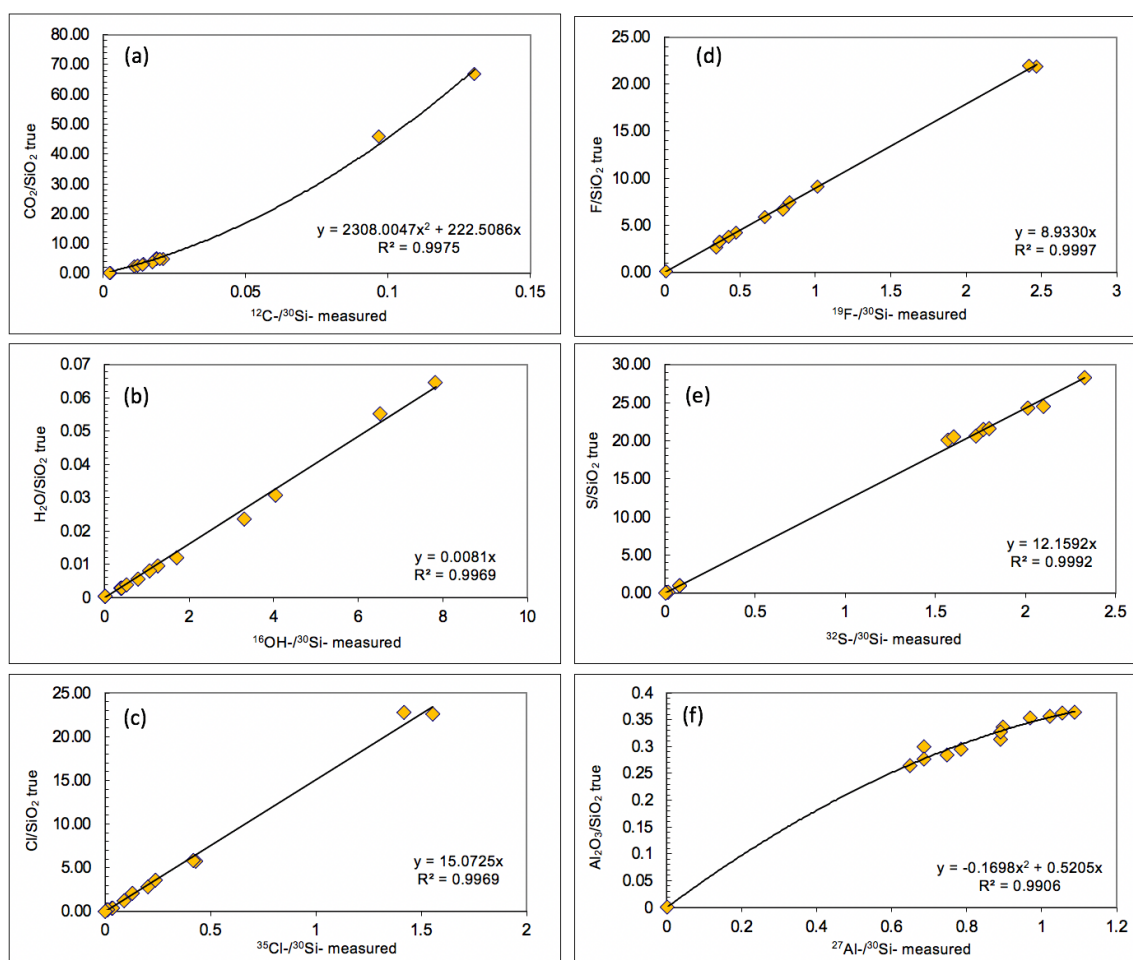
Supplementary Figure S2. Google maps (© Google Maps 2023) of (A) SV location relative to the city of Naples, the town of Pompeii and the Campi Flegrei Caldera, and of (B) sample locations studied in this work.



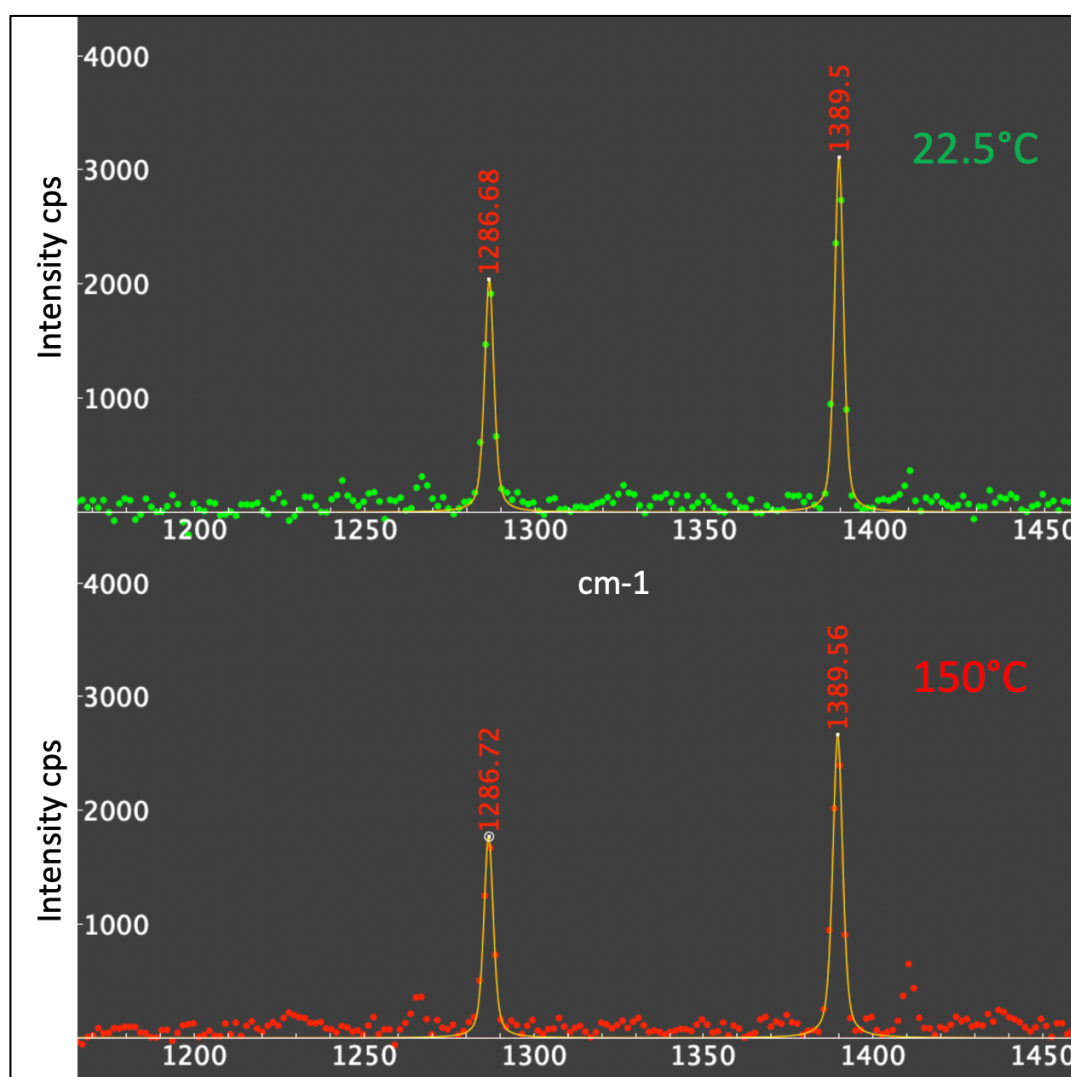
Supplementary Figure S3. Synthetic scheme of eruption timelines at SV based on Megacycles and explosivity of eruptions (Plinian versus Inter-Plinian); modified after De Vivo et al. (2010). Ages are as reported by Santacroce et al. (2008; and references therein).



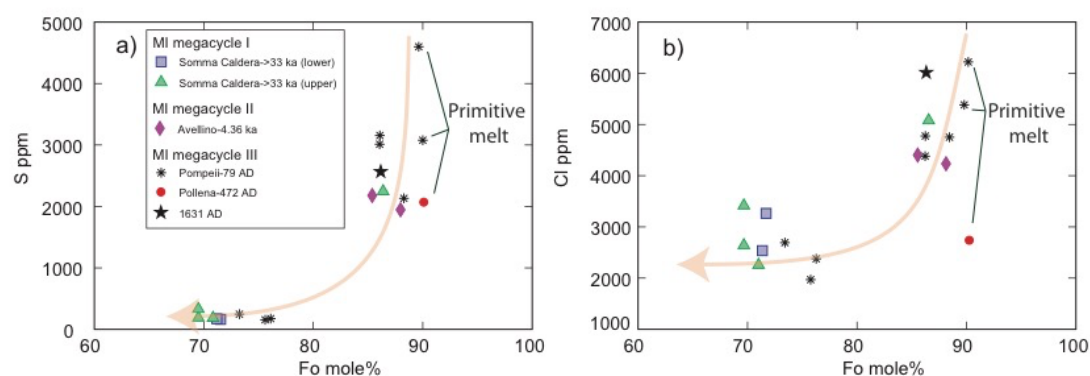
Supplementary Figure S4. Photomicrograph of a MI showing a decrepitation halo. The MI is hosted in olivine from sample SCL12 (pre-Codola lava sample). The photomicrograph was taken after the MI was reheated, no photomicrographs were taken before the heating experiment, and it is not possible to establish if the decrepitation halo developed during the heating experiment.



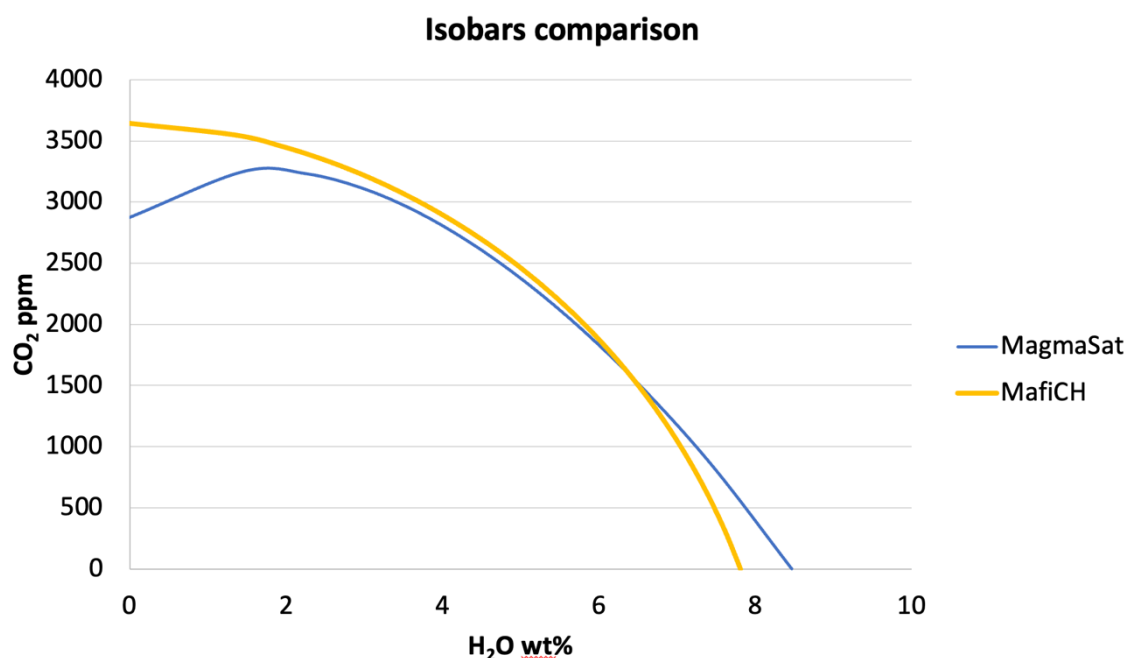
Supplementary Figure S5. SIMS calibration curves developed and used for the volatile concentrations reported for the MI of this study. a) $^{12}\text{C}/^{30}\text{Si}$ measured versus CO_2/SiO_2 true ratios based on glass references used for the SIMS working session. b) $^{16}\text{OH}/^{30}\text{Si}$ measured versus $\text{H}_2\text{O}/\text{SiO}_2$ true ratios based on glass references used for the SIMS working session. c) $^{35}\text{Cl}/^{30}\text{Si}$ measured versus Cl/SiO_2 true ratios based on glass references used for the SIMS working session. d) $^{19}\text{F}/^{30}\text{Si}$ measured versus Cl/SiO_2 true ratios based on glass references used for the SIMS working session. e) $^{32}\text{S}/^{30}\text{Si}$ measured versus S/SiO_2 true ratios based on glass references used for the SIMS working session. f) $^{27}\text{Al}/^{30}\text{Si}$ measured versus $\text{Al}_2\text{O}_3/\text{SiO}_2$ true ratios based on glass references used for the SIMS working session. The data point for each glass reference represents 5 different spots measured in 10 cycles depth mode. Details concerning the glass references used for these calibration curves are reported in *Auxiliary Table A3*.



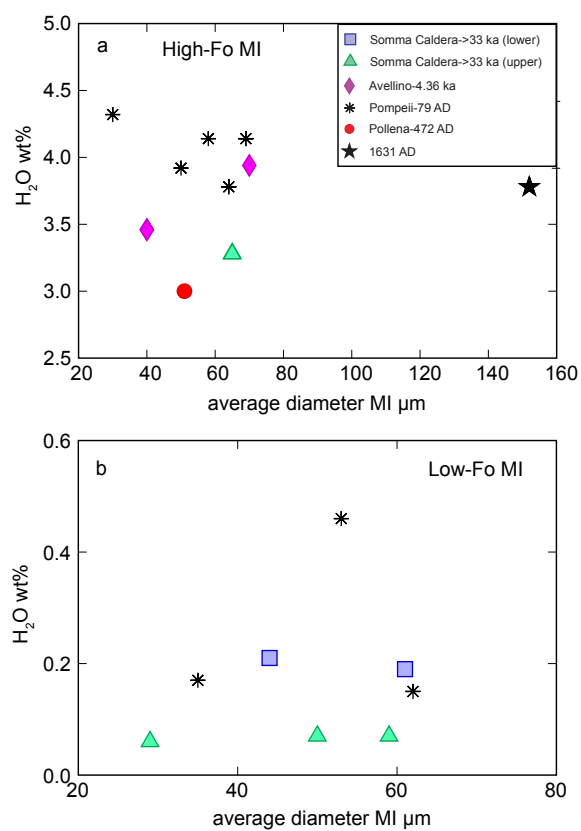
Supplementary Figure S6. Comparison of CO_2 Fermi diad peaks of the same bubble (LFL2-D44-3-2; Avellino eruption) taken at different temperatures at the same depth from the surface (Esposito et al., 2016). Upper panel shows the CO_2 Fermi diads at room T (22.5°C), while the bottom panel shows CO_2 Fermi diad at 150°C.



Supplementary Figure S7. Correlation between Fo content (mole%) of the host and volatile contents of MI hosted in olivine from this study. a) Fo mole% versus S discriminated by single eruptions. b) Fo mole% versus Cl discriminated by single eruptions. MI that represent primitive or near-primitive melts below SV hosted in olivine with Fo₉₀ are highlighted.



Supplementary Figure S8. Comparison between the 400 MPa isobar calculated by MafiCH solubility model (Allison et al., 2022) and that calculated by MagmaSat (Ghiorso and Gualda, 2015). The isobars were calculated assuming MI LFL2-D44-1-1 as the starting major element composition. For the isobar calculated by MagmaSat, a temperature of 1200°C and an NNO buffer were assumed.



Supplementary Figure S9. Melt inclusion diameter vs. uncorrected H₂O contents of MI to test for H-loss from MI by diffusion before eruption. a) MI size vs. H₂O contents of Fo-rich MI. b) MI size vs. H₂O contents of Fo-poor MI. H₂O contents of MI shown here are not corrected for H-diffusive loss and PEC. Note the different scales on the axes of both panels.